Gapped Collective Charge Excitations and Interlayer Hopping in Cuprate Superconductors

M. Hepting,[1,*] M. Bejas,[2] A. Nag,[3] H. Yamase,[4,5] N. Coppola,[6] D. Betto,[1] C. Falter,[7] M. Garcia-Fernandez,[3] S. Agrestini,[3] Ke-Jin Zhou,[3] M. Minola,[1] C. Sacco,[6] L. Maritato,[6,8] P. Orgiani,[8,9] H. I. Wei,[10] K. M. Shen,[10] D. G. Schlom,[11,12,13] A. Galdi,[6,14] A. Greco,[2,†] and B. Keimer[1]

[1]*Max-Planck-Institute for Solid State Research, Heisenbergstraße 1, 70569 Stuttgart, Germany*
[2]*Facultad de Ciencias Exactas, Ingeniería y Agrimensura and Instituto de Física de Rosario (UNR-CONICET), Avenida Pellegrini 250, 2000 Rosario, Argentina*
[3]*Diamond Light Source, Harwell Campus, Didcot OX11 0DE, United Kingdom*
[4]*International Center of Materials Nanoarchitectonics, National Institute for Materials Science, Tsukuba 305-0047, Japan*
[5]*Department of Condensed Matter Physics, Graduate School of Science, Hokkaido University, Sapporo 060-0810, Japan*
[6]*Dipartimento di Ingegneria Industriale, Università di Salerno, I-84084 Fisciano (Salerno), Italy*
[7]*Institut für Festkörpertheorie, Westfälische Wilhelms-Universität, Wilhelm-Klemm-Straße 10, 48149 Münster, Germany*
[8]*CNR-SPIN Salerno, Università di Salerno, I-84084 Fisciano (Salerno), Italy*
[9]*CNR-IOM, TASC Laboratory in Area Science Park, 34139 Trieste, Italy*
[10]*LASSP, Department of Physics, Cornell University, Ithaca, New York 14853, USA*
[11]*Department of Materials Science and Engineering, Cornell University, Ithaca, New York 14853, USA*
[12]*Kavli Institute at Cornell for Nanoscale Science, Ithaca, New York 14853, USA*
[13]*Leibniz-Institut für Kristallzüchtung, Max-Born-Straße 2, 12489 Berlin, Germany*
[14]*Cornell Laboratory for Accelerator Based Sciences and Education, Cornell University, Ithaca, New York 14853, USA*

(Received 24 September 2021; revised 29 March 2022; accepted 28 June 2022; published 19 July 2022)

We use resonant inelastic x-ray scattering to probe the propagation of plasmons in the electron-doped cuprate superconductor $Sr_{0.9}La_{0.1}CuO_2$. We detect a plasmon gap of ∼120 meV at the two-dimensional Brillouin zone center, indicating that low-energy plasmons in $Sr_{0.9}La_{0.1}CuO_2$ are not strictly acoustic. The plasmon dispersion, including the gap, is accurately captured by layered *t-J-V* model calculations. A similar analysis performed on recent resonant inelastic x-ray scattering data from other cuprates suggests that the plasmon gap is generic and its size is related to the magnitude of the interlayer hopping t_z. Our work signifies the three dimensionality of the charge dynamics in layered cuprates and provides a new method to determine t_z.

DOI: 10.1103/PhysRevLett.129.047001

A variety of enigmatic states emerge in layered cuprates upon hole doping or electron doping, such as the pseudogap, charge order, strange metal, and—most prominently—high-temperature superconductivity [1,2]. While it is widely believed that antiferromagnetic spin fluctuations play a key role in the superconducting pairing [3–8], it is not yet established whether the spin channel alone is responsible for the superconductivity in cuprates. For instance, the relevance of electron-phonon coupling is still under debate [9–15], and theoretical studies propose that low-energy plasmons [16–22] or plasmon-phonon modes [23,24] mediate superconductivity in cuprates, or contribute constructively to the high superconducting transition temperature T_c [25,26]. Irrespective of the specific type of pairing glue, Anderson and co-workers suggested that T_c is not a single-plane property [27] and interlayer Josephson tunneling of Cooper pairs strongly amplifies the T_c of cuprates [28,29], which was discussed controversially in subsequent studies [30–36]. The interlayer tunneling mechanism is most effective when coherent single particle hopping between adjacent CuO_2 planes is inhibited in the normal state [28]. Nevertheless, coherent normal-state *c*-axis transport properties were detected in various experiments on overdoped cuprates [37–39], while in lightly doped cuprates it is challenging to assess whether interlayer hopping is small or absent [37,40]. In fact, the extraction of accurate values of the interlayer hopping integral t_z from experimental data has proven difficult not only for lightly but also for overdoped cuprates [38,41–45]. Hence, the t_z determined from first-principle calculations [46,47] is frequently employed, which was suggested to be

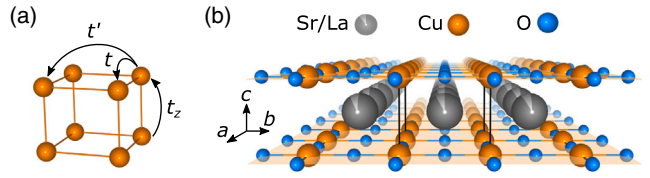

FIG. 1. (a) Schematic of the hopping integrals t, t', and t_z on a stacked square lattice. (b) Schematic of the crystal structure of $Sr_{0.9}La_{0.1}CuO_2$ (SLCO). Solid black lines correspond to the crystallographic unit cell. CuO_2 planes are indicated in orange.

as large as t' or $0.1t$ in some cuprates [47], with t' and t denoting the in-plane next-nearest and nearest neighbor hopping, respectively [Fig. 1(a)]. In contrast, other studies assume that t_z is negligibly small compared to t' and t, which is in line with a smaller interlayer hopping evaluated from experiments [40,42]. Thus, new methods for a reliable determination of the contentious parameter t_z are highly desirable.

Notably, recent theoretical work has emphasized that the interlayer hopping is also encoded in the plasmon spectrum of cuprates and should manifest as a gap at the two-dimensional (2D) Brillouin zone (BZ) center [48]. More specifically, in layered systems, such as the cuprates, the plasmon dispersion (for small q) neither follows a $\sqrt{q}$ dependence that is typical for 2D metals, nor the q^2 behavior of isotropic 3D metals [49–51]. Instead, poorly screened interlayer Coulomb interaction between the CuO_2 planes gives rise to a plasmon spectrum containing a set of acoustic branches, which disperse linearly for small q, and one optical branch [17]. In the presence of interlayer charge transfer, however, the former plasmon branches are not strictly acoustic, but gapped at the 2D BZ center. Yet, while seemingly acoustic plasmons were identified in recent resonant inelastic x-ray scattering (RIXS) experiments on various electron- and hole-doped cuprates [52–55] including $La_{1.825}Ce_{0.175}CuO_4$ (LCCO) and $La_{1.84}Sr_{0.16}CuO_4$ (LSCO), a gap has not been observed unambiguously.

In this Letter, we study plasmon excitations in the electron-doped cuprate $Sr_{0.9}La_{0.1}CuO_2$ (SLCO), which exhibits the infinite-layer crystal structure. Using RIXS, we detect an energy gap of the acousticlike modes at the in-plane BZ center. The observed plasmon dispersion, including the gap, is accurately captured by t-J-V model calculations, and characteristic microscopic parameters, such as t_z, are determined. The application of our analysis scheme to previously published RIXS data of other cuprates suggests considerably smaller plasmon gaps and interlayer hoppings in LCCO and LSCO.

The RIXS measurements were performed on a SLCO thin film with a superconducting transition temperature $T_c \sim 30$ K and a thickness of 294 Å grown by molecular-beam epitaxy on a (110) oriented $TbScO_3$ substrate [56]. Figure 1(b) shows the crystal structure of SLCO, which exhibits CuO_2 planes stacked along the c-axis direction with La/Sr spacer layers, which corresponds to the infinite-layer structure [57,58]. The lattice constants $a, b = 3.960$ Å and $c = 3.405$ Å were determined by x-ray diffraction. Note that for SLCO the interlayer distance is equivalent to the c-axis lattice constant, whereas in LCCO the interlayer distance corresponds to $c/2 \sim 6.05$ Å [52].

All RIXS spectra were collected at the Cu L_3 edge with high energy resolution ($\Delta E \approx 40$ meV) at $T = 20$ K at the I21-RIXS beamline of the Diamond Light Source, UK [59]. The momentum resolution was $\Delta q \approx 0.01$ Å^{-1} [59]. A similar scattering geometry as in Ref. [54] was employed, with the a/b axis and the c axis of SLCO lying in the scattering plane and incident photons linearly polarized perpendicular to the scattering plane (σ polarization). Importantly, the continuous rotation of the RIXS spectrometer arm allowed for a variation of the scattering angle, and the corresponding rotation of the sample enabled the independent variation of the in-plane ($q_\parallel$) and out-of-plane momentum transfer (q_z). In the following we denote the momentum transfer by (H, K, L) in reciprocal lattice units $(2\pi/a, 2\pi/b, 2\pi/c)$.

Figure 2(a) shows a representative set of RIXS spectra for different in-plane momenta H. The spectra were fitted by the sum of the elastic line at zero-energy loss and several damped harmonic oscillator functions accounting for inelastic features. Details about the fitting procedure, assignment of the features, and the complete set of spectra are given in the Supplemental Material [60]. As the most relevant features, we identify (i) an essentially nondispersive peak around 95 meV, (ii) a paramagnon peak around 190 meV for $|H| \geq 0.06$, and (iii) a fast dispersive peak with an energy higher than 120 meV [Figs. 2(a) and 2(b)]. We attribute the 95 meV feature to a high-energy (HE) phonon. While phonons in cuprates are typically observed below 85 meV [76–78], zone-boundary phonons with energies as high as 91.4 meV were predicted for the infinite-layer cuprate $SrCuO_2$ [79]. The further increase of phonon energy in our SLCO film could be due to the epitaxial strain induced by the substrate or the La doping. The assignment of the paramagnon peak (see Supplemental Material [60]) is in line with Ref. [80], which investigated the paramagnon dispersion in a similar SLCO film, but focused on large in-plane momenta and employed a lower energy resolution of $\Delta E = 265$ meV. In contrast to the paramagnon, the fast dispersing peak exhibits substantial spectral intensity at the zone center $H = 0$ [Figs. 2(a) and 2(b)]. Close inspection of the spectra with small H reveals that the peak likely also contains contributions from the HE phonon, which precludes unambiguous fitting for $|H| \leq 0.005$. Nevertheless, we emphasize that the center of gravity of the superposed peak [labeled as plasmon in Figs. 2(a) and 2(b)] exceeds 120 meV even at $H = 0$, indicating the presence of an energy gap for this mode. Notably, a charge origin of the fast dispersing mode was already proposed in the low-resolution measurements in

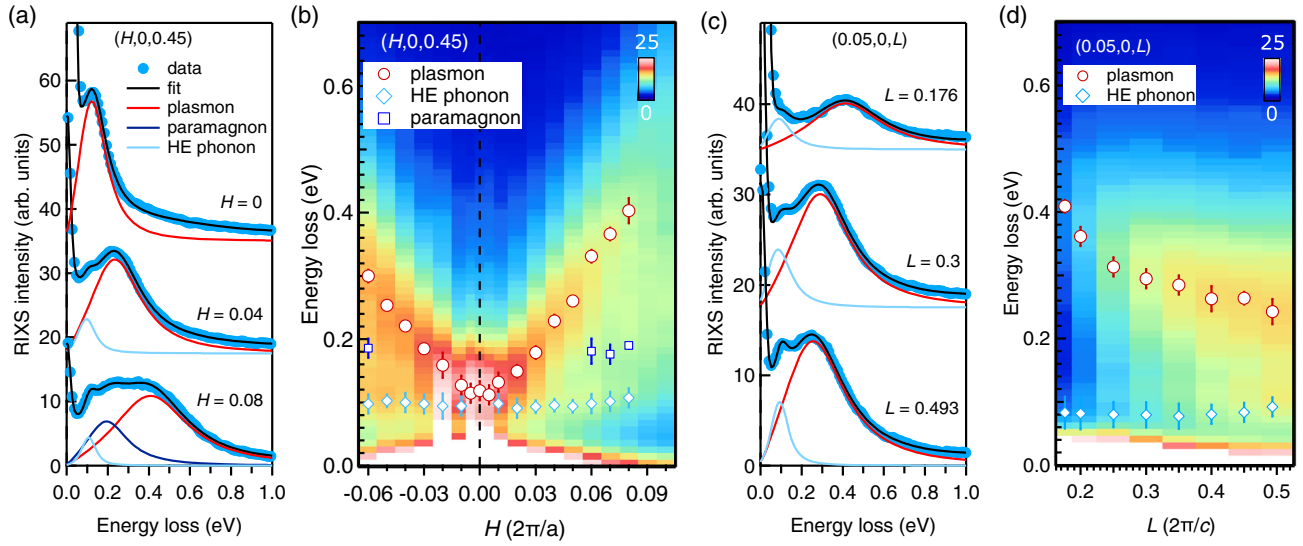

FIG. 2. (a) Vertically stacked RIXS spectra for representative momenta along the $(H, 0, 0.45)$ direction. Solid black lines are fits to the spectra. Fitted peak profiles of the plasmon, paramagnon, and high-energy (HE) phonon are shown, while the other contributions to the fit are omitted for clarity (for details of the fitting procedure see Supplemental Material [60]). (b) RIXS intensity map for momenta along the $(H, 0, 0.45)$ direction. Open symbols are peak positions extracted from fits. The color scale of the map is capped at 25 arb. units (white color). (c) Vertically stacked RIXS spectra for representative momenta along the $(0.05, 0, L)$ direction. (d) RIXS intensity map for momenta along the $(0.05, 0, L)$ direction.

Ref. [80], while a gap around $H = 0$ was not resolved and the investigation of a possible dispersion along L was lacking. As shown in Figs. 2(c) and 2(d), our high-resolution measurement reveals that the peak exhibits a distinctive dispersion as a function of L. Along the lines of Refs. [52,54], such L dependence with a minimum around $L = 0.5$ identifies the mode as an acoustic plasmon excitation. On the other hand, the H dependence in Fig. 2(b) shows that the mode exhibits a gap of ~120 meV at $H = 0$. Thus, the seemingly acoustic plasmons in SLCO are not strictly acoustic, but gapped. This observation calls for a thorough theoretical investigation of the emergence and the energy scale of the gap, which we present next.

Previously, typical properties of the plasmons in cuprates were studied by random phase approximation (RPA) calculations [17,25,49,55,81], a combination of determinant quantum Monte Carlo and RPA in a layered Hubbard model [52], an extended variational wave function approach [82], and a large-N theory of the layered t-J-V model [48,83,84]. In the following, we turn to the latter theory, which emphasized in Ref. [48] that acoustic plasmons in cuprates are not strictly acoustic, but exhibit an energy gap at the 2D BZ center. The t-J model is widely employed as an effective model for cuprates [85] and accounts for strong correlations. Importantly, the t-J-V model includes not only first-nearest-neighbor (t), second-nearest-neighbor (t'), and interlayer (t_z) hoppings [Fig. 1(a)], but also the long-range Coulomb interaction $V(\mathbf{q})$ (see Supplemental Material [60]), which is crucial given the three-dimensional character of plasmons in layered cuprates [52]. Figure 3(a) shows the imaginary part of the charge susceptibility $\chi_c''(\mathbf{q}, \omega)$ computed in the framework of a large-N theory of the t-J-V model for doping $\delta = 0.1$ and a broadening parameter $\Gamma/t = 0.1$, which is required to account for the experimental resolution and a possible broadening due to correlations [86]. All other fit components (see Supplemental Material [60]) were subtracted from the RIXS spectrum in Fig. 3(a) to make a direct comparison with $\chi_c''(\mathbf{q}, \omega)$. To capture the full plasmon dispersion in SLCO, we have applied an error minimization fitting procedure for the t-J-V model (see Supplemental Material [60]), using the experimentally determined plasmon peak positions [Figs. 2(b) and 2(d)] as an input. Figures 3(b) and 3(c) show the computed plasmon branches as a function of momenta H and L, respectively, together with corresponding experimental data. Note that the experimentally determined peak positions for $|H| \leq 0.005$ [gray symbols in Figs. 3(b) and 3(d)] with a strong overlap with the HE phonon were excluded from the fitting procedure for the t-J-V model, to avoid any bias in the determination of a gap at the 2D BZ center. Besides the measured plasmon branches along the $(H, 0, 0.45)$ and $(0.05, 0, L)$ directions, additional calculated branches for unmeasured H and L values are shown in Figs. 3(b) and 3(c), respectively. The obtained spectrum of plasmon modes, including the optical branch for $L = 0$, is qualitatively reminiscent of previous calculations for cuprates [17,25,52,81], but additionally features a distinct energy gap at $H, K = 0$ [Fig. 3(b)], which is along the lines of calculations in Refs. [48,54,82–84].

Figure 3(d) focuses on small in-plane momenta around the observed plasmon gap at the 2D BZ center and

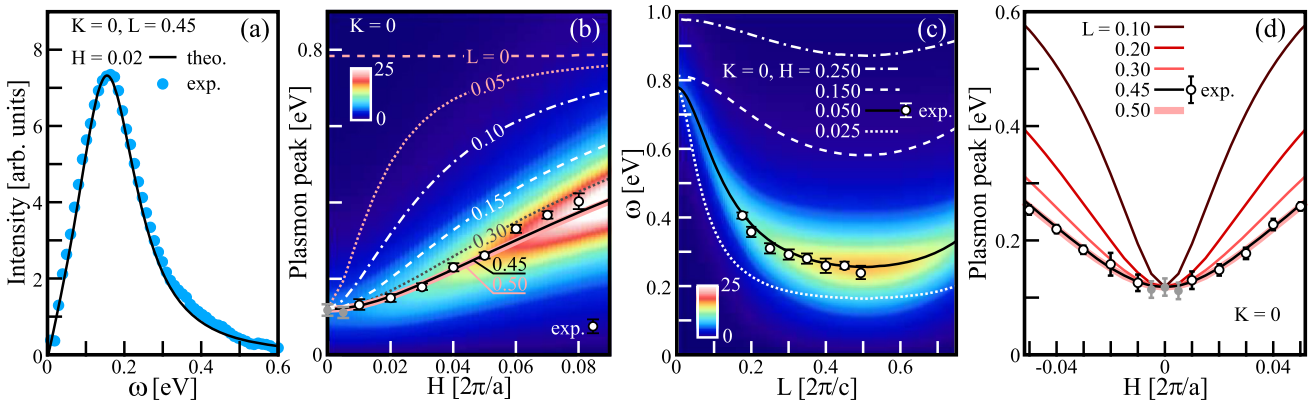

FIG. 3. (a) Imaginary part of the charge susceptibility $\chi_c''(\mathbf{q},\omega)$ for momentum (0.02,0,0.45) (solid black line) computed in the layered t-J-V model. Superimposed are experimental data (blue symbols), which correspond to the plasmon component in the RIXS raw data. The intensity of $\chi_c''(\mathbf{q},\omega)$ is scaled such that it fits to the maximum of the RIXS data. (b) Computed intensity map of $\chi_c''(\mathbf{q},\omega)$ for momenta along the $(H,0,0.45)$ direction. The solid black line corresponds to the maxima of $\chi_c''(\mathbf{q},\omega)$. The other lines indicate the maxima of $\chi_c''(\mathbf{q},\omega)$ computed for different L. Experimental plasmon peak positions for momenta along the $(H,0,0.45)$ direction are superimposed as white and gray symbols. The former symbols correspond to peak positions used as an input for the fitting procedure for the t-J-V model, while the latter were not included (see text). (c) Computed intensity map and maxima for different H along the $(0.05,0,L)$ direction. (d) Computed plasmon dispersion around the 2D BZ center at $H=0$ for different L.

illustrates the excellent agreement between experiment and theory. As the key result of our study, the fitting with the t-J-V model yields $t_z/t = 0.055$ (corresponding to $t_z = 55$ meV, see Supplemental Material) for the interlayer hopping. This is in line with $t_z/t = 0.06$, determined by first-principles calculations for $CaCuO_2$ [87], which is a closely related infinite-layer cuprate. Moreover, we obtain the in-plane and out-of-plane dielectric constants $\epsilon_\parallel/\epsilon_0 = 5.89$ and $\epsilon_\perp/\epsilon_0 = 1.06$ from the t-J-V model fitting, which are similar to theoretical predictions for infinite-layer cuprates [79]. We emphasize that a gap with a magnitude of ~120 meV is a robust feature, which is rooted in the presence of a finite t_z [48] and cannot be attributed exclusively to other effects, such as the broadening Γ. In fact, in absence of interlayer hopping, Γ can induce only a relatively small gap in SLCO (see Supplemental Material [60]).

As a next step, we apply the present fitting procedure for the t-J-V model to other systems and revisit previous RIXS data on LCCO and LSCO reported in Refs. [52,54], respectively. Note that in the case of LCCO the gap was estimated to be approximately zero [52], while in LSCO the previous analysis with the t-J-V model indicated 75 meV as an upper limit [54]. The present analysis (see Supplemental Material [60]) indicates an upper limit of 82 meV for the gap in LCCO and 55 meV for LSCO, which are both substantially smaller than the gap size in SLCO. While the strength of the Coulomb interaction is comparable in the three cuprates, a particularly strong interlayer hopping can be expected in the latter compound due to its distinct infinite-layer crystal structure with narrowly spaced adjacent CuO_2 planes [Fig. 1(b)], thus rationalizing the large gap value of more than 100 meV, which in turn enabled our first conclusive observation of a plasmon gap with RIXS.

The corresponding hoppings t_z/t for the upper limits of the plasmon gaps in LCCO and LSCO are 0.03 ($t_z = 30$ meV) and 0.01 ($t_z = 7$ meV), respectively. Employing a larger t_z/t of 0.1 for LSCO [47] would yield a large gap of 344 meV with the present methodology. This suggests that the interlayer hopping in LSCO is indeed very small and motivates future RIXS studies with higher resolution to determine the value of the gap in LSCO experimentally. Furthermore, we estimate the lower bound of the plasmon gap by assuming a hypothetical $t_z = 0$, leading to 58 and 41 meV for LCCO and LSCO, respectively. These lower bounds arise purely from the broadening Γ (see Supplemental Material [60]).

Having established the plasmon gap at the 2D BZ center in different cuprates, we next focus on the plasmon properties for nonzero in-plane momentum transfer. A close inspection of the H dependence of the dispersion in the vicinity of $H = 0$ in LCCO and LSCO [52,54] reveals that the intensity of the plasmon peak decreases when approaching the 2D BZ center. This behavior is also expected from the t-J-V model calculations [Fig. 3(b)]. For SLCO, a similar trend might not be obvious in the RIXS intensity map in Fig. 2(b), due to the overlap with the paramagnon, phonons, and the elastic line. Nevertheless, a plot of the fitted integrated intensity of the plasmon peak as a function of H reveals that also SLCO exhibits a comparable trend (see Supplemental Material [60])—except for momenta $|H| \leq 0.005$ where a sharp increase of the intensity occurs. This increase is likely a result of the superposition of the plasmon and the HE phonon peak, but cannot be disentangled unambiguously in the present RIXS

data owing to an insufficient energy resolution. Future higher-resolution RIXS experiments might be capable of resolving the different spectral components around $H = 0$ in SLCO, and are also desirable for LSCO, where a coupling between the plasmon and a c-axis polarized phonon mode of apical oxygen ions was predicted for small momenta, with an expected gap of the mixed plasmon-phonon mode of ∼60 meV [24]. Note that in SLCO, however, plasmon-phonon coupling can be ruled out (see Supplemental Material [60]).

In summary, our observation and theoretical description of the plasmon gap provide the missing piece of the puzzle alongside the q_z dependence [52,54,55] to consolidate the 3D character of plasmons in cuprates. This gap was neither evidenced in previous optical spectroscopy [88] nor electron-energy loss spectroscopy (EELS) studies [89], yet its unambiguous presence underscores the importance of explicit inclusion of the interlayer hopping t_z for a comprehensive description of the charge dynamics of cuprates. On a fundamental level, the charge degrees of freedom and the dynamics of the normal state are considered as a prerequisite for understanding the superconducting state [36]. Hence, in a broader context, the presence of a substantial plasmon gap at the 2D BZ center calls for a reassessment of the theories proposing that acoustic plasmons mediate superconductivity [16–22] and raise the T_c of cuprates as much as 20% [25]. In particular, it should be evaluated whether the gap energy has a positive or negative effect in the suggested pairing scenarios. Along the lines of previous discussions about a correlation between T_c and the magnitude of t' [90], future applications of our methodology may provide new insights into a possible relation between T_c and t_z, as well as the putative scaling of T_c with the number of CuO_2 planes per unit cell [91,92]. In this context, we note that the large-N theory for the t-J-V model indicates that the doping dependence of the plasmon gap exhibits a domelike shape [48], similar to the T_c dome of cuprates [1]. Nevertheless, detailed calculations are required to assess the impact of a gap on the value of T_c, considering not only the electron self-energy, but also vertex corrections, as the relatively large energy scale of the plasmon may invalidate Migdal's theorem [93].

More specifically, our approach combining RIXS and t-J-V model calculations enables the extraction of robust values of t_z in cuprates—possibly even in lightly doped cuprates which has not been accomplished with other experimental methods [40–44]. Moreover, we anticipate that our methodology will be applicable to other materials, including layered 2D materials and van der Waals heterostructures [94–96], as well as the newly discovered infinite-layer nickelate superconductors [97–99], which might possess even larger interlayer hoppings than SLCO [87].

We thank A. V. Boris and P. Horsch for fruitful discussions, and W. Metzner for a critical reading of the manuscript. A. Greco acknowledges the Max-Planck-Institute for Solid State Research in Stuttgart for hospitality and financial support. H. Y. was supported by JSPS KAKENHI Grant No. JP20H01856, Japan. K. M. S. and H. I. W. acknowledge support from the Air Force Office of Scientific Research through Grant No. FA9550-21-1-0168. D. G. S. acknowledges support from the National Science Foundation (NSF) under Grant No. DMR-1610781. We acknowledge Diamond Light Source for providing the beamtime under the proposal MM23933.

*hepting@fkf.mpg.de
†agreco@fceia.unr.edu.ar

[1] B. Keimer, S. A. Kivelson, M. R. Norman, S. Uchida, and J. Zaanen, From quantum matter to high-temperature superconductivity in copper oxides, Nature (London) **518**, 179 (2015).
[2] N. P. Armitage, P. Fournier, and R. L. Greene, Progress and perspectives on electron-doped cuprates, Rev. Mod. Phys. **82**, 2421 (2010).
[3] P. A. Lee, N. Nagaosa, and X.-G. Wen, Doping a Mott insulator: Physics of high-temperature superconductivity, Rev. Mod. Phys. **78**, 17 (2006).
[4] D. J. Scalapino, A common thread: The pairing interaction for unconventional superconductors, Rev. Mod. Phys. **84**, 1383 (2012).
[5] P. Dai, H. A. Mook, R. D. Hunt, and F. Doğan, Evolution of the resonance and incommensurate spin fluctuations in superconducting $YBa_2Cu_3O_{6+x}$, Phys. Rev. B **63**, 054525 (2001).
[6] M. Le Tacon *et al.*, Intense paramagnon excitations in a large family of high-temperature superconductors, Nat. Phys. **7**, 725 (2011).
[7] M. P. M. Dean, G. Dellea, R. S. Springell, F. Yakhou-Harris, K. Kummer, N. B. Brookes, X. Liu, Y.-J. Sun, J. Strle, T. Schmitt, L. Braicovich, G. Ghiringhelli, I. Božović, and J. P. Hill, Persistence of magnetic excitations in $La_{2-x}Sr_xCuO_4$ from the undoped insulator to the heavily overdoped non-superconducting metal, Nat. Mater. **12**, 1019 (2013).
[8] D. Vilardi, C. Taranto, and W. Metzner, Antiferromagnetic and d-wave pairing correlations in the strongly interacting two-dimensional Hubbard model from the functional renormalization group, Phys. Rev. B **99**, 104501 (2019).
[9] J. P. Franck, Experimental studies of the isotope effect in high temperature superconductors, in *Physical Properties of High Temperature Superconductors IV*, edited by D. M. Ginsberg (World Scientific, Singapore, 1994).
[10] T. Cuk, F. Baumberger, D. H. Lu, N. Ingle, X. J. Zhou, H. Eisaki, N. Kaneko, Z. Hussain, T. P. Devereaux, N. Nagaosa, and Z.-X. Shen, Coupling of the B_{1g} Phonon to the Antinodal Electronic States of $Bi_2Sr_2Ca_{0.92}Y_{0.08}Cu_2O_{8+\delta}$, Phys. Rev. Lett. **93**, 117003 (2004).
[11] R. Heid, R. Zeyher, D. Manske, and K.-P. Bohnen, Phonon-induced pairing interaction in $YBa_2Cu_3O_7$ within the local-density approximation, Phys. Rev. B **80**, 024507 (2009).
[12] F. Giustino, M. L. Cohen, and S. G. Louie, Small phonon contribution to the photoemission kink in the copper oxide superconductors, Nature (London) **452**, 975 (2008).

[13] D. Reznik, G. Sangiovanni, O. Gunnarsson, and T. P. Devereaux, Photoemission kinks and phonons in cuprates, Nature (London) **455**, E6 (2008).

[14] E. G. Maksimov, M. L. Kulić, and O. V. Dolgov, Bosonic spectral function and the electron-phonon interaction in HTSC cuprates, Adv. Condens. Matter Phys. **2010**, 1 (2010).

[15] S. Johnston, F. Vernay, B. Moritz, Z.-X. Shen, N. Nagaosa, J. Zaanen, and T. P. Devereaux, Systematic study of electron-phonon coupling to oxygen modes across the cuprates, Phys. Rev. B **82**, 064513 (2010).

[16] J. Ruvalds, Plasmons and high-temperature superconductivity in alloys of copper oxides, Phys. Rev. B **35**, 8869 (1987).

[17] V. Z. Kresin and H. Morawitz, Layer plasmons and high-T_c superconductivity, Phys. Rev. B **37**, 7854 (1988).

[18] S.-M. Cui and C.-H. Tsai, Plasmon theory of high-T_c superconductivity, Phys. Rev. B **44**, 12500 (1991).

[19] Y. Ishii and J. Ruvalds, Acoustic plasmons and cuprate superconductivity, Phys. Rev. B **48**, 3455 (1993).

[20] Y. M. Malozovsky, S. M. Bose, P. Longe, and J. D. Fan, Eliashberg equations and superconductivity in a layered two-dimensional metal, Phys. Rev. B **48**, 10504 (1993).

[21] D. Varshney and R. K. Singh, Superconductivity in lanthanum cuprates: A layered-electron-gas model, Phys. Rev. B **52**, 7629 (1995).

[22] E. Pashitskii and V. Pentegov, On the plasmon mechanism of high-T_c superconductivity in layered crystals and two-dimensional systems, J. Low Temp. Phys. **34**, 113 (2008).

[23] C. Falter and M. Klenner, Nonadiabatic and nonlocal electron-phonon interaction and phonon-plasmon mixing in the high-temperature superconductors, Phys. Rev. B **50**, 9426 (1994).

[24] T. Bauer and C. Falter, Impact of dynamical screening on the phonon dynamics of metallic La_2CuO_4, Phys. Rev. B **80**, 094525 (2009).

[25] A. Bill, H. Morawitz, and V. Z. Kresin, Electronic collective modes and superconductivity in layered conductors, Phys. Rev. B **68**, 144519 (2003).

[26] A. Grankin and V. Galitski, Interplay of hyperbolic plasmons and superconductivity, arXiv:2201.07731.

[27] P. W. Anderson, Experimental constraints on the theory of high-T_c superconductivity, Science **256**, 1526 (1992).

[28] S. Chakravarty, A. Sudbø, P. W. Anderson, and S. Strong, Interlayer tunneling and gap anisotropy in high-temperature superconductors, Science **261**, 337 (1993).

[29] P. W. Anderson, Interlayer tunneling mechanism for high-T_c superconductivity: Comparison with c axis infrared experiments, Science **268**, 1154 (1995).

[30] A. J. Leggett, Interlayer tunneling models of cuprate superconductivity: Implications of a recent experiment, Science **274**, 587 (1996).

[31] A. A. Tsvetkov, D. van der Marel, K. A. Moler, J. R. Kirtley, J. L. de Boer, A. Meetsma, Z. F. Ren, N. Koleshnikov, D. Dulic, A. Damascelli, M. Grüninger, J. Schützmann, J. W. van der Eb, H. S. Somal, and J. H. Wang, Global and local measures of the intrinsic Josephson coupling in $Tl_2Ba_2CuO_6$ as a test of the interlayer tunnelling model, Nature (London) **395**, 360 (1998).

[32] K. A. Moler, J. R. Kirtley, D. G. Hinks, T. W. Li, and M. Xu, Images of interlayer josephson vortices in $Tl_2Ba_2CuO_{6+\delta}$, Science **279**, 1193 (1998).

[33] P. W. Anderson, c-axis electrodynamics as evidence for the interlayer theory of high-temperature superconductivity, Science **279**, 1196 (1998).

[34] J. R. Kirtley, K. A. Moler, G. Villard, and A. Maignan, c-Axis Penetration Depth of Hg-1201 Single Crystals, Phys. Rev. Lett. **81**, 2140 (1998).

[35] S. Chakravarty, H.-Y. Kee, and E. Abrahams, Frustrated Kinetic Energy, the Optical Sum Rule, and the Mechanism of Superconductivity, Phys. Rev. Lett. **82**, 2366 (1999).

[36] D. N. Basov, S. I. Woods, A. S. Katz, E. J. Singley, R. C. Dynes, M. Xu, D. G. Hinks, C. C. Homes, and M. Strongin, Sum rules and interlayer conductivity of high-T_c cuprates, Science **283**, 49 (1999).

[37] S. Uchida, K. Tamasaku, and S. Tajima, c-axis optical spectra and charge dynamics in $La_{2-x}Sr_xCuO_4$, Phys. Rev. B **53**, 14558 (1996).

[38] N. E. Hussey, M. Abdel-Jawad, A. Carrington, A. P. Mackenzie, and L. A. Balicas, A coherent three-dimensional Fermi surface in a high-transition-temperature superconductor, Nature (London) **425**, 814 (2003).

[39] C. C. Homes, S. V. Dordevic, D. A. Bonn, R. Liang, W. N. Hardy, and T. Timusk, Coherence, incoherence, and scaling along the c axis of $YBa_2Cu_3O_{6+x}$, Phys. Rev. B **71**, 184515 (2005).

[40] H. Yamase, Y. Sakurai, M. Fujita, S. Wakimoto, and K. Yamada, Fermi surface in La-based cuprate superconductors from Compton scattering imaging, Nat. Commun. **12**, 2223 (2021).

[41] T. Takeuchi, T. Kondo, T. Kitao, H. Kaga, H. Yang, H. Ding, A. Kaminski, and J. C. Campuzano, Two- to Three-Dimensional Crossover in the Electronic Structure of $(Bi,Pb)_2(Sr,La)_2CuO_{6+\delta}$ from Angle-Resolved Photoemission Spectroscopy, Phys. Rev. Lett. **95**, 227004 (2005).

[42] M. Horio *et al.*, Three-Dimensional Fermi Surface of Overdoped La-Based Cuprates, Phys. Rev. Lett. **121**, 077004 (2018).

[43] C. E. Matt *et al.*, Direct observation of orbital hybridisation in a cuprate superconductor, Nat. Commun. **9**, 972 (2018).

[44] Y. Zha, S. L. Cooper, and D. Pines, Model of c-axis resistivity of high-T_c cuprates, Phys. Rev. B **53**, 8253 (1996).

[45] G. Grissonnanche, Y. Fang, A. Legros, S. Verret, F. Laliberté, C. Collignon, J. Zhou, D. Graf, P. A. Goddard, L. Taillefer, and B. J. Ramshaw, Linear-in temperature resistivity from an isotropic Planckian scattering rate, Nature (London) **595**, 667 (2021).

[46] O. Andersen, A. Liechtenstein, O. Jepsen, and F. Paulsen, LDA energy bands, low-energy Hamiltonians, t', t'', $t_\perp(k)$, and $J_\perp$, J. Phys. Chem. Solids **56**, 1573 (1995).

[47] R. S. Markiewicz, S. Sahrakorpi, M. Lindroos, H. Lin, and A. Bansil, One-band tight-binding model parametrization of the high-T_c cuprates including the effect of k_z dispersion, Phys. Rev. B **72**, 054519 (2005).

[48] A. Greco, H. Yamase, and M. Bejas, Plasmon excitations in layered high-T_c cuprates, Phys. Rev. B **94**, 075139 (2016).

[49] D. Grecu, Plasma frequency of the electron gas in layered structures, Phys. Rev. B **8**, 1958 (1973).

[50] A. L. Fetter, Electrodynamics of a layered electron gas. II. Periodic array, Ann. Phys. (N.Y.) **88**, 1 (1974).

[51] D. Grecu, Self-consistent field approximation for the plasma frequencies of an electron gas in a layered thin film, J. Phys. C **8**, 2627 (1975).

[52] M. Hepting *et al.*, Three-dimensional collective charge excitations in electron-doped copper oxide superconductors, Nature (London) **563**, 374 (2018).

[53] J. Lin, J. Yuan, K. Jin, Z. Yin, G. Li, K.-J. Zhou, X. Lu, M. Dantz, T. Schmitt, H. Ding, H. Guo, M. P. M. Dean, and X. Liu, Doping evolution of the charge excitations and electron correlations in electron-doped superconducting $La_{2-x}Ce_xCuO_4$, npj Quantum Mater. **5**, 4 (2020).

[54] A. Nag, M. Zhu, M. Bejas, J. Li, H. C. Robarts, H. Yamase, A. N. Petsch, D. Song, H. Eisaki, A. C. Walters, M. García-Fernández, A. Greco, S. M. Hayden, and K.-J. Zhou, Detection of Acoustic Plasmons in Hole-Doped Lanthanum and Bismuth Cuprate Superconductors Using Resonant Inelastic X-Ray Scattering, Phys. Rev. Lett. **125**, 257002 (2020).

[55] A. Singh, H. Y. Huang, C. Lane, J. H. Li, J. Okamoto, S. Komiya, R. S. Markiewicz, A. Bansil, T. K. Lee, A. Fujimori, C. T. Chen, and D. J. Huang, Acoustic plasmons and conducting carriers in hole-doped cuprate superconductors, Phys. Rev. B **105**, 235105 (2022).

[56] A. Galdi, P. Orgiani, C. Sacco, B. Gobaut, P. Torelli, C. Aruta, N. B. Brookes, M. Minola, J. W. Harter, K. M. Shen, D. G. Schlom, and L. Maritato, X-ray absorption spectroscopy study of annealing process on $Sr_{1-x}La_xCuO_2$ electron-doped cuprate thin films, J. Appl. Phys. **123**, 123901 (2018).

[57] P. Fournier, T' and infinite-layer electron-doped cuprates, Physica (Amsterdam) **514C**, 314 (2015).

[58] J. Tomaschko, S. Scharinger, V. Leca, J. Nagel, M. Kemmler, T. Selistrovski, D. Koelle, and R. Kleiner, Phase-sensitive evidence for $d_{x^2-y^2}$-pairing symmetry in the parent-structure high-T_c cuprate superconductor $Sr_{1-x}La_xCuO_2$, Phys. Rev. B **86**, 094509 (2012).

[59] K.-J. Zhou, A. Walters, M. Garcia-Fernandez, T. Rice, M. Hand, A. Nag, J. Li, S. Agrestini, P. Garland, H. Wang, S. Alcock, I. Nistea, B. Nutter, N. Rubies, G. Knap, M. Gaughran, F. Yuan, P. Chang, J. Emmins, and G. Howell, I21: An advanced high-resolution resonant inelastic x-ray scattering beamline at diamond light source, J. Synchrotron Radiat. **29**, 563 (2022).

[60] See Supplemental Material at http://link.aps.org/supplemental/10.1103/PhysRevLett.129.047001 for details of the RIXS raw data and fits, theoretical scheme, fitting procedure in the t-J-V model, broadening Γ, possible plasmon gap in LCCO and LSCO, intensity of the plasmon, and plasmon-phonon coupling, which includes Refs. [60–74].

[61] R. Fumagalli, L. Braicovich, M. Minola, Y. Y. Peng, K. Kummer, D. Betto, M. Rossi, E. Lefrançois, C. Morawe, M. Salluzzo, H. Suzuki, F. Yakhou, M. Le Tacon, B. Keimer, N. B. Brookes, M. M. Sala, and G. Ghiringhelli, Polarization-resolved Cu L_3-edge resonant inelastic x-ray scattering of orbital and spin excitations in $NdBa_2Cu_3O_{7-\delta}$, Phys. Rev. B **99**, 134517 (2019).

[62] M. Minola, G. Dellea, H. Gretarsson, Y. Y. Peng, Y. Lu, J. Porras, T. Loew, F. Yakhou, N. B. Brookes, Y. B. Huang, J. Pelliciari, T. Schmitt, G. Ghiringhelli, B. Keimer, L. Braicovich, and M. Le Tacon, Collective Nature of Spin Excitations in Superconducting Cuprates Probed by Resonant Inelastic X-Ray Scattering, Phys. Rev. Lett. **114**, 217003 (2015).

[63] T. Thio, T. R. Thurston, N. W. Preyer, P. J. Picone, M. A. Kastner, H. P. Jenssen, D. R. Gabbe, C. Y. Chen, R. J. Birgeneau, and A. Aharony, Antisymmetric exchange and its influence on the magnetic structure and conductivity of La_2CuO_4, Phys. Rev. B **38**, 905 (1988).

[64] A. Foussats and A. Greco, Large-N expansion based on the Hubbard operator path integral representation and its application to the t-J model. II. The case for finite J, Phys. Rev. B **70**, 205123 (2004).

[65] F. Becca, M. Tarquini, M. Grilli, and C. Di Castro, Charge-density waves and superconductivity as an alternative to phase separation in the infinite-U Hubbard-Holstein model, Phys. Rev. B **54**, 12443 (1996).

[66] M. Bejas, H. Yamase, and A. Greco, Dual structure in the charge excitation spectrum of electron-doped cuprates, Phys. Rev. B **96**, 214513 (2017).

[67] M. S. Hybertsen, E. B. Stechel, M. Schluter, and D. R. Jennison, Renormalization from density-functional theory to strong-coupling models for electronic states in Cu-O materials, Phys. Rev. B **41**, 11068 (1990).

[68] E. J. Singley, D. N. Basov, K. Kurahashi, T. Uefuji, and K. Yamada, Electron dynamics in $Nd_{1.85}Ce_{0.15}CuO_{4+\delta}$: Evidence for the pseudogap state and unconventional c-axis response, Phys. Rev. B **64**, 224503 (2001).

[69] M. Suzuki, Hall coefficients and optical properties of $La_{2-x}Sr_xCuO_4$ single-crystal thin films, Phys. Rev. B **39**, 2312 (1989).

[70] S. Uchida, T. Ido, H. Takagi, T. Arima, Y. Tokura, and S. Tajima, Optical spectra of $La_{2-x}Sr_xCuO_4$: Effect of carrier doping on the electronic structure of the CuO_2 plane, Phys. Rev. B **43**, 7942 (1991).

[71] C. Falter, M. Klenner, and G. Hoffmann, Screening and phonon-plasmon scenario as calculated from a realistic electronic bandstructure based on LDA for La_2CuO_4, Phys. Status Solidi B **209**, 235 (1998).

[72] L. Pintschovius, Electron-phonon coupling effects explored by inelastic neutron scattering, Phys. Status Solidi B **242**, 30 (2005).

[73] V. W. Brar, M. S. Jang, M. Sherrott, S. Kim, J. J. Lopez, L. B. Kim, M. Choi, and H. Atwater, Hybrid surface-phonon-plasmon polariton modes in graphene/monolayer h-BN heterostructures, Nano Lett. **14**, 3876 (2014).

[74] R. J. Koch, T. Seyller, and J. A. Schaefer, Strong phonon-plasmon coupled modes in the graphene/silicon carbide heterosystem, Phys. Rev. B **82**, 201413(R) (2010).

[75] F. J. Bezares, A. D. Sanctis, J. R. M. Saavedra, A. Woessner, P. Alonso-González, I. Amenabar, J. Chen, T. H. Bointon, S. Dai, M. M. Fogler, D. N. Basov, R. Hillenbrand, M. F. Craciun, F. J. García de Abajo, S. Russo, and F. H. L. Koppens, Intrinsic plasmon-phonon interactions in highly doped graphene: A near-field imaging study, Nano Lett. **17**, 5908 (2017).

[76] O. Gunnarsson and O. Rösch, Interplay between electron–phonon and Coulomb interactions in cuprates, J. Phys. Condens. Matter **20**, 043201 (2008).
[77] S. Koval and R. Migoni, Lattice dynamics of the infinite-layered compounds, Physica (Amsterdam) **257C**, 255 (1996).
[78] M.-O. Mun, Y. S. Roh, J. H. Kim, C. Jung, J. Kim, and S.-I. Lee, Optical phonons of superconducting infinite-layer compounds $Sr_{0.9}Ln_{0.1}CuO_2$ (Ln = La and Sm), Physica (Amsterdam) **364C–365C**, 629 (2001).
[79] M. Klenner, C. Falter, and Q. Chen, Calculated phonon dispersion of infinite-layer compounds and the effects of charge fluctuations, Z. Phys. B **95**, 417 (1994).
[80] G. Dellea, M. Minola, A. Galdi, D. Di Castro, C. Aruta, N. B. Brookes, C. J. Jia, C. Mazzoli, M. Moretti Sala, B. Moritz, P. Orgiani, D. G. Schlom, A. Tebano, G. Balestrino, L. Braicovich, T. P. Devereaux, L. Maritato, and G. Ghiringhelli, Spin and charge excitations in artificial hole- and electron-doped infinite layer cuprate superconductors, Phys. Rev. B **96**, 115117 (2017).
[81] R. S. Markiewicz, M. Z. Hasan, and A. Bansil, Acoustic plasmons and doping evolution of Mott physics in resonant inelastic x-ray scattering from cuprate superconductors, Phys. Rev. B **77**, 094518 (2008).
[82] M. Fidrysiak and J. Spałek, Unified theory of spin and charge excitations in high-T_c cuprate superconductors: A quantitative comparison with experiment and interpretation, Phys. Rev. B **104**, L020510 (2021).
[83] A. Greco, H. Yamase, and M. Bejas, Origin of high-energy charge excitations observed by resonant inelastic x-ray scattering in cuprate superconductors, Commun. Phys. **2**, 3 (2019).
[84] A. Greco, H. Yamase, and M. Bejas, Close inspection of plasmon excitations in cuprate superconductors, Phys. Rev. B **102**, 024509 (2020).
[85] F. C. Zhang and T. M. Rice, Effective Hamiltonian for the superconducting Cu oxides, Phys. Rev. B **37**, 3759 (1988).
[86] P. Prelovšek and P. Horsch, Electron-energy loss spectra and plasmon resonance in cuprates, Phys. Rev. B **60**, R3735 (1999).
[87] A. S. Botana and M. R. Norman, Similarities and Differences between $LaNiO_2$ and $CaCuO_2$ and Implications for Superconductivity, Phys. Rev. X **10**, 011024 (2020).
[88] I. Bozovic, Plasmons in cuprate superconductors, Phys. Rev. B **42**, 1969 (1990).
[89] J. Fink, M. Knupfer, S. Atzkern, and M. Golden, Electronic correlations in solids, studied using electron energy-loss spectroscopy, J. Electron Spectrosc. Relat. Phenom. **117–118**, 287 (2001).
[90] E. Pavarini, I. Dasgupta, T. Saha-Dasgupta, O. Jepsen, and O. K. Andersen, Band-Structure Trend in Hole-Doped Cuprates and Correlation with $T_{c\,\max}$, Phys. Rev. Lett. **87**, 047003 (2001).
[91] A. Iyo, Y. Tanaka, H. Kito, Y. Kodama, P. M. Shirage, D. D. Shivagan, H. Matsuhata, K. Tokiwa, and T. Watanabe, T_c vs n relationship for multilayered high-T_c superconductors, J. Phys. Soc. Jpn. **76**, 094711 (2007).
[92] G. Vincini, S. Tajima, S. Miyasaka, and K. Tanaka, Multi-layer effects in $Bi_2Sr_2Ca_2Cu_3O_{10+z}$ superconductors, Supercond. Sci. Technol. **32**, 113001 (2019).
[93] G. D. Mahan, *Many-Particle Physics*, 2nd ed. (Plunum Press, New York, 1990).
[94] P. Cudazzo, M. Gatti, and A. Rubio, Plasmon dispersion in layered transition-metal dichalcogenides, Phys. Rev. B **86**, 075121 (2012).
[95] R. E. Groenewald, M. Rösner, G. Schönhoff, S. Haas, and T. O. Wehling, Valley plasmonics in transition metal dichalcogenides, Phys. Rev. B **93**, 205145 (2016).
[96] K. S. Thygesen, Calculating excitons, plasmons, and quasiparticles in 2D materials and van der Waals heterostructures, 2D Mater. **4**, 022004 (2017).
[97] D. Li, K. Lee, B. Wang, M. Osada, S. Crossley, H. Lee, Y. Cui, Y. Hikita, and H. Hwang, Superconductivity in an infinite-layer nickelate, Nature (London) **572**, 624 (2019).
[98] M. Hepting *et al.*, Electronic structure of the parent compound of superconducting infinite-layer nickelates, Nat. Mater. **19**, 381 (2020).
[99] S. Zeng, C. Li, L. E. Chow, Y. Cao, Z. Zhang, C. S. Tang, X. Yin, Z. S. Lim, J. Hu, P. Yang, and A. Ariando, Superconductivity in infinite-layer nickelate $La_{1-x}Ca_xNiO_2$ thin films, Sci. Adv. **8**, eabl9927 (2022).